Insect-Pathogen Dynamics: Stage-Specific Susceptibility and Insect Density Dependence

M. MOERBEEK AND F. VAN DEN BOSCH*
*Department of Mathematics, Agricultural University, Dreijenlaan 4,
6703 HA Wageningen, The Netherlands*

ABSTRACT

The control of insect pests by using insect pathogens as dynamic biological control agents is a recent effort. Model studies on insect-pathogen relations can help in the development of biocontrol programs. Except for the work of Briggs and Godfray [1], insect-pathogen models ignore the stage-specific susceptibility of insects. Moreover most models do not incorporate insect self-regulation. We develop stage-structured models of insect-pathogen relations incorporating insect-density dependence and disease transmitted through direct contact between susceptible and infective individuals. The models are analyzed by using steady-state and stability analysis. Numerical solutions are used as sources of further insight into the dynamics of the insect-pathogen systems. It is shown that there are major differences in the dynamics of adult- and juvenile-infecting diseases. Moreover, the interplay between insect-density dependence and stage-specific susceptibility has important consequences for the dynamics of insect-pathogen systems. © Elsevier Science Inc., 1997

1. INTRODUCTION

Insect pests are a serious threat in many agricultural and forestry systems. One seeks to control insect populations by applying synthetic insecticides in many situations. For reasons of environmental safety, research has focused on methods to drive back the use of these synthetic insecticides. Methods have been developed to control insect populations by using natural enemies of the pest insect. Such biological control programs usually make use of parasitoids or predators. The use of these organisms is now well established and operationalized for the control of several insect pests. A more recent effort is the use of insect pathogens as biological control agents. The use of insect pathogens has focused on the development of microbial agents or products that are

---

*Author to whom correspondence should be addressed.

applied as "natural" insecticides [2, 3]. Recently, however, researchers have begun to explore the use of insect pathogens as dynamic biological control agents [4-9]. Using pathogens for biological control requires an understanding of the dynamics of insect pathogens and their interaction with the dynamics of the pest species.

The first efforts toward understanding the dynamics of insect-pathogen interactions date to the eighties. Population ecologists led by Anderson and May [10, 11] discovered the capability of regulation of insect populations by pathogens. They developed and analyzed seven model variants. For these models, they calculated threshold parameter values for disease persistence, steady states of the insect population density, and stability of the steady states. Their modelling study was followed by several other model approaches considering the effect of various aspects of a pathogen's life history.

Model studies of insect-pathogen interactions can be classified on the bases of transmission dynamics of the disease and the presence of insect-density dependence. Many fungal and viral insect diseases kill the infected host, followed by the release of infective particles into the environment [2]. Susceptible hosts become infected through encounters with these free-living infective stages. To study these diseases, the dynamics of the density of the free-living infective stage in the environment is modeled, and the rate of infection of susceptibles is assumed to depend on susceptible density and infective-stage density [1, 10-12, 13]. Other authors assume disease transmission to depend on the product of the density of susceptible and infective individuals [11, 14-16]. This assumption is more appropriate for insect diseases in which the infectious agent is short lived outside the host or for diseases that are transmitted directly between host individuals. Examples of such diseases are those caused by various nematodes, some sexually transmitted, and protozoa, as well as some bacterial and fungal diseases with short-lived transmission stages [2, 5, 6].

In most models, the insect population is assumed to grow exponentially in the absence of disease [1, 11, 13, 16]. This assumption is appropriate in some agricultural systems where one seeks to control the insect below the crop-damage threshold. Below the damage threshold, the insect population is far below carrying capacity, and exponential growth is a good approximation. In other agricultural and forestry systems and in field populations, the extensive defoliation that occurs argues that self-limitation of the insect population has to be taken into account [15, 17]. It has been shown that insect-density dependence has major consequences for the dynamics of the insect-pathogen system. On the basis of a model without insect-density dependence, Anderson and May [10] claimed that the cyclic dynamics observed in forest insects

results from insect-pathogen dynamics. Bowers et al. [15], however, showed that incorporating insect-density−dependence cycles is less likely. Moreover, using parameter estimates from field data usually fails to generate population cycles. Begon et al. [14] showed that insect-density dependence is important in host-host-pathogen systems. Incorporating insect-density−dependence coexistence of hosts is more likely than in the absence of insect self-regulation.

   Models of insect-pathogen systems usually ignore the feature of stage dependent susceptibility well known in insects. Depending on the pathogen and the insect species either the juvenile stage or the adult stage is susceptible [2, 3, 5, 18]. In a recent paper, Briggs and Godfray [1] showed that stage-dependent susceptibility strongly affects the dynamics of insect pathogen systems. They modeled insect pathogens transmitted through a free-living infective stage. In their models, they did not incorporate insect-density dependence. The objective of this paper is twofold. First, we investigate the effects of stage-dependent susceptibility for insect diseases with direct transmission. Second, we address the question of the effect of insect-density dependence in stage-structured models. It will be shown that the interplay between stage-dependent susceptibility and insect-density dependence has unexpected effects on the dynamics of insect-pathogen systems.

2. THE MODELS

2.1. *THE INSECT POPULATION WITHOUT INFECTIOUS DISEASE*

   We model an insect population consisting of two life stages: juveniles and adults. The density of juveniles in the population, $J(t)$, increases owing to birth, $b(t)$, and decreases owing to maturation into the adult stage, $M(t)$, and owing to death. The density of adults, $A(t)$, increases owing to the maturation of juveniles and decreases owing to death. We assume a constant death rate, ω_J and ω_A, for J and A, respectively. The dynamics of J and A are governed by the differential equations

$$\frac{dJ}{dt} = b(t) - M(t) - \omega_J J,$$

$$\frac{dA}{dt} = M(t) - \omega_A A. \tag{1}$$

We assume resources of adults and juveniles to be different. This assumption is realistic for most insect species. Birth rate then depends only on adult density. The per capita birthrate of adult insects is denoted by $E(t)$. Thus,

$$b(t) = E(t)A(t). \tag{2}$$

Following Gurney et al. [19], we model the dependence of the per capita birth rate of adult insects as

$$E = \gamma e^{-\xi A}, \tag{3}$$

where γ is the rate of offspring production per adult individual at infinitesimally low adult density and ξ measures the effect of adult population density on reproduction. This exponential dependence of the per capita reproductive output is found in several data sets; for example, see [20, 21]. The total population birth rate thus takes the form

$$b(t) = \gamma A(t) e^{-\xi A(t)}. \tag{4}$$

This dependence of population birth rate on population density is known as the Ricker equation. It is assumed that juveniles mature into the adult stage at a fixed age τ. The maturation rate thus is

$$M(t) = b(t - \tau)P, \tag{5}$$

where P is the probability that a juvenile survives until age τ. Because, in the model, death rate is constant,

$$P = e^{-\omega_j \tau}. \tag{6}$$

This completes the specification of the model for the insect population without an infectious disease. This model was developed and analyzed by Gurney et al. [22]. They showed that this simple time-delayed model gives good qualitative as well as quantitive agreement with Nicholson's classic blowfly experiments. It explains, among other things, the appearance of single-generation cycles in blowfly populations.

2.2. THE INFECTIOUS DISEASE

The insects are susceptible to an infectious disease. The disease is infective to one of the life stages. We assume the disease to be of the classical Susceptible, Infective and Removed (SIR) type. Furthermore, we make the simplifying assumption that an infected individual suffers from the disease such that it does not take part in the dynamics of the insect population. More specifically, in the case of adult diseases, birth rate depends only on the density of uninfected adults; for juvenile diseases, infected juveniles do not mature into the adult stage.

2.3. THE ADULT DISEASE

In our first model, the adult individuals are susceptible to an infectious disease. The rate at which adults become infected is proportional to the product of the density of susceptible adults, $A(t)$, and the density

of infected adults, $I(t)$, with proportionality α. This constant α will be called the transmission coefficient. Infected adults die at constant rate β. The death rate, β, is the sum of the "natural death rate" not due to disease, which is equal for susceptible and infected individuals, and the disease-induced death rate. Therefore, a reasonable biological constraint on β is $\beta \geq \omega_A$. The model thus reads

$$\frac{dJ}{dt} = b(t) - b(t-\tau)P(t) - \omega_J J,$$

$$\frac{dA}{dt} = b(t-\tau)P(t) - \omega_A A - \alpha IA, \tag{7}$$

$$\frac{dI}{dt} = \alpha IA - \beta I,$$

where $b(t)$ and P are given by Equations (4) and (6), respectively.

2.4. *THE JUVENILE DISEASE*

In our second model, the juvenile individuals are susceptible to an infectious disease. The rate at which juveniles become infected is proportional to the density of susceptible juveniles, $J(t)$, and the density of infected juveniles, $I(t)$, with proportionality constant α, the transmission coefficient. Infected juveniles die at constant rate β. This death rate, β, is the sum of the "natural death rate" not due to disease and the disease-induced death rate. Therefore, the biological constraint on β is $\beta \geq \omega_J$. The model thus reads

$$\frac{dJ}{dt} = b(t) - b(t-\tau)P(t) - \omega_J J - \alpha IJ,$$

$$\frac{dA}{dt} = b(t-\tau)P(t) - \omega_A A, \tag{8}$$

$$\frac{dI}{dt} = \alpha IJ - \beta I,$$

where $b(t)$ is given by Equation (4). In this model, the probability of surviving until adulthood, $P(t)$, depends not only on the juvenile death rate ω_J, but also on the rate of infection due to the disease. Consider a group of susceptible juveniles, $N(t)$, born at time $t = t^*$. The rate of change in the number of susceptibles is given by

$$\frac{dN(t)}{dt} = -[\omega_J + \alpha I(t)]N(t). \tag{9}$$

Integrating from $t = t^*$ to t, we find

$$N(t) = N(t^*)e^{-\int_{t^*}^{t}\{\omega_J + \alpha I(\sigma)\}d\sigma}. \tag{10}$$

Juveniles maturing at time t were born at time $t - \tau$, and the probability of surviving until adulthood takes the form

$$P(t) = \frac{N(t)}{N(t - \tau)} = e^{-\int_{t-\tau}^{t} \{\omega_J + \alpha I(\sigma)\} d\sigma}. \tag{11}$$

2.5. THE NONSTAGE STRUCTURE EQUIVALENT

To be able to separate the effects of insect-density dependence from the effects of stage-specific susceptibility, we also study the nonstage structured variant

$$\frac{dS}{dt} = \gamma S e^{-\xi S} - \omega S - \alpha SI,$$

$$\tag{12}$$

$$\frac{dI}{dt} = \alpha SI - \beta I,$$

where S is insect density, ω is the death rate not due to disease, and β is the sum of the death rate not due to disease and the death rate due to disease. Again, α is the transmission coefficient.

2.6. SCALING THE MODELS

Variables in both models are scaled by using

$$A^* = \xi A, \quad J^* = \xi J, \quad I^* = \xi I, \quad t^* = \gamma t, \tag{13}$$

and, for the nonstage-structured equivalent, $S^* = \xi S$. Further, we define the scaled parameters as

$$\alpha^* = \frac{\alpha}{\xi \gamma}, \quad \omega_J^* = \frac{\omega_J}{\gamma}, \quad \omega_A^* = \frac{\omega_A}{\gamma}, \quad \beta^* = \frac{\beta}{\gamma}, \quad \tau^* = \gamma \tau, \tag{14}$$

and, for the nonstage-structured variant $\omega^* = \omega / \gamma$. These scaled variables and constants are substituted in the models, and the suffix is dropped. The model of an insect population without infectious disease yields the scaled equations

$$\frac{dJ}{dt} = A e^{-A} - A(t - \tau) e^{-A(t-\tau)} e^{-\omega_J \tau} - \omega_J J,$$

$$\tag{15}$$

$$\frac{dA}{dt} = A(t - \tau) e^{-A(t-\tau)} e^{-\omega_J \tau} - \omega_A A;$$

for the model of an adult disease, we find the equations

$$\frac{dJ}{dt} = Ae^{-A} - A(t-\tau)e^{-A(t-\tau)}e^{-\omega_J\tau} - \omega_J J,$$

$$\frac{dA}{dt} = A(t-\tau)e^{-A(t-\tau)}e^{-\omega_J\tau} - \omega_A A - \alpha IA, \qquad (16)$$

$$\frac{dI}{dt} = \alpha IA - \beta I;$$

for the model of a juvenile disease,

$$\frac{dJ}{dt} = Ae^{-A} - A(t-\tau)e^{-A(t-\tau)}P(t) - \omega_J J - \alpha IJ,$$

$$\frac{dA}{dt} = A(t-\tau)e^{-A(t-\tau)}P(t) - \omega_A A, \qquad (17)$$

$$\frac{dI}{dt} = \alpha IJ - \beta I,$$

where $\quad P(t) = e^{-\int_{t-\tau}^{t}\{\omega_J + \alpha I(\sigma)\}d\sigma}$;

and, for the nonstage-structured model,

$$\frac{dS}{dt} = Se^{-S} - \omega S - \alpha S,$$

$$\frac{dI}{dt} = \alpha SI - \beta I. \qquad (18)$$

For use in the discussion of results, we note that the scaled population total birth rate [Eq. (4)] becomes

$$b(t) = Ae^{-A}. \qquad (19)$$

The population birth rate reaches a maximum at $A = 1$ and decreases with further increase of A.

These four models (Sections 2.3–2.6) will be the subject of our analysis in Section 3, 4 and 5. For the model of the insect population without infectious disease, we will quote the results of Gurney et al. [19], for use in the analysis of the other models.

3. STEADY STATES

3.1. *THE INSECT POPULATION WITHOUT INFECTIOUS DISEASE*

From Equations (15) we find a trivial steady state,

$$\left(\hat{J}_1, \hat{A}_1\right) = (0,0), \qquad (20)$$

and the internal steady state

$$\left(\hat{J}_2, \hat{A}_2\right) = \left[\frac{\omega_A}{\omega_J}(\ln \omega_A + \omega_J\tau)(1 - e^{\omega_J\tau}), -\ln \omega_A - \omega_J\tau\right]. \quad (21)$$

A steady state is biologically relevant only if its value is larger than or equal to zero. The steady state of Equation (21) exists, in this biological sense, if

$$\frac{1}{\omega_A}e^{-\omega_J\tau} > 1. \quad (22)$$

This combination of parameters has a clear biological interpretation. Consider one newly born individual in the density-independent situation. The probability that this juvenile survives until adulthood equals $\exp\{-\omega_J\tau\}$. The average time span in which this individual can reproduce is $1/\omega_A$. Recall the scaling and note that the rate of offspring produced per adult at low population density equals one. Thus $(1/\omega_A)\exp\{-\omega_J\tau\}$ is the average number of offspring produced per individual in the density-independent situation. This quantity is known in ecology as the net-reproductive number, $R_{0,\text{insect}} = (1/\omega_A) \exp\{-\omega_J\tau\}$. If the net-reproductive number is larger than one, the animal species can invade a virgin habitat and, as a consequence, the internal steady state exists.

3.2. THE ADULT DISEASE

Besides the trivial steady state

$$\left(\hat{J}_1, \hat{A}_1, \hat{I}_1\right) = (0,0,0), \quad (23)$$

we find the boundary steady state $(\hat{J}_2, \hat{A}_2, \hat{I}_2) = (\hat{J}_2, \hat{A}_2, 0)$, where $\hat{J}_2$ and $\hat{A}_2$ are given by Equation (21). This steady state has the same interpretation as that for the model of the insect population without infectious disease.

The third steady state, the internal steady state, is given by

$$\left(\hat{J}_3, \hat{A}_3, \hat{I}_3\right) = \left[\frac{\beta}{\alpha\omega_J}e^{-\frac{\beta}{\alpha}}(1 - e^{-\omega_J\tau}), \frac{\beta}{\alpha}, \frac{1}{\alpha}\left(e^{-\frac{\beta}{\alpha} - \omega_J\tau} - \omega_A\right)\right]. \quad (24)$$

This steady state exists, in a biological sense, if

$$\frac{\alpha}{\beta}(-\ln \omega_A - \omega_J\tau) > 1. \quad (25)$$

The term in parentheses is the steady-state adult density in a population without the infectious disease present, $\hat{A}_2$. The average lifetime of an infected individual is $1/\beta$, in which it produces on average $\alpha\hat{A}_2$ new infections per unit of time. The parameter combination on the left-hand side of Inequality (25) can thus be interpreted as the average number of new infections produced by one infected adult at infinitesimally low density of infected individuals, the net-reproductive number of the disease, $R_{0,\,\text{disease}} = (\alpha/\beta)(-\ln\omega_A - \omega_J\tau)$. It is obvious that the infectious disease can invade the animal population when $R_{0,\,\text{disease}}$ is larger than unity.

Figure 1 shows the steady-state values of juveniles, susceptible adults, and infected adults as a function of the transmission coefficient, α, for two sets of values of the other parameters. The branch of internal steady states bifurcates supercritically from the branch of boundary steady states at $R_{0,\,\text{disease}}$. Susceptible-adult density decreases and infected-adult density increases with increasing transmission coefficient, which is biologically plausible. Combining the two graphs reveals that total adult density decreases with increasing transmission coefficient, α. Juvenile density either decreases or increases with transmission coefficient. These phenomena hinge upon the Ricker-type dependence of the population birth rate on susceptible-adult density. From Equation (24), we find

$$\frac{d\hat{J}_3}{d\alpha} > (<)0 \quad \Leftrightarrow \quad \frac{\beta}{\alpha} > (<)1. \tag{26}$$

Because β/α is the steady-state susceptible-adult density, this inequality implies that juvenile density decreases with α if susceptible-adult density is smaller than unity. Recalling the scaled Ricker equation [Eq. (19)], we can conclude that juvenile density increases when population birth rate decreases owing to the susceptible-adult density being larger than unity. Consideration of the change in juvenile density with transmission coefficient close to $R_{0,\,\text{disease}} = 1$ can be a source of further insight. From

$$\left.\frac{d\hat{J}_3}{d\alpha}\right|_{R_{0,\text{disease}}-1} > 0 \quad \Leftrightarrow \quad -\ln\omega_A - \omega_J\tau > 1 \quad \Leftrightarrow \quad \hat{A}_2 > 1, \tag{27}$$

it follows that, for diseases with net reproduction close to unity, juvenile density increases when the adult density of a population without the infectious disease is larger than the density where the Ricker equation has its maximum.
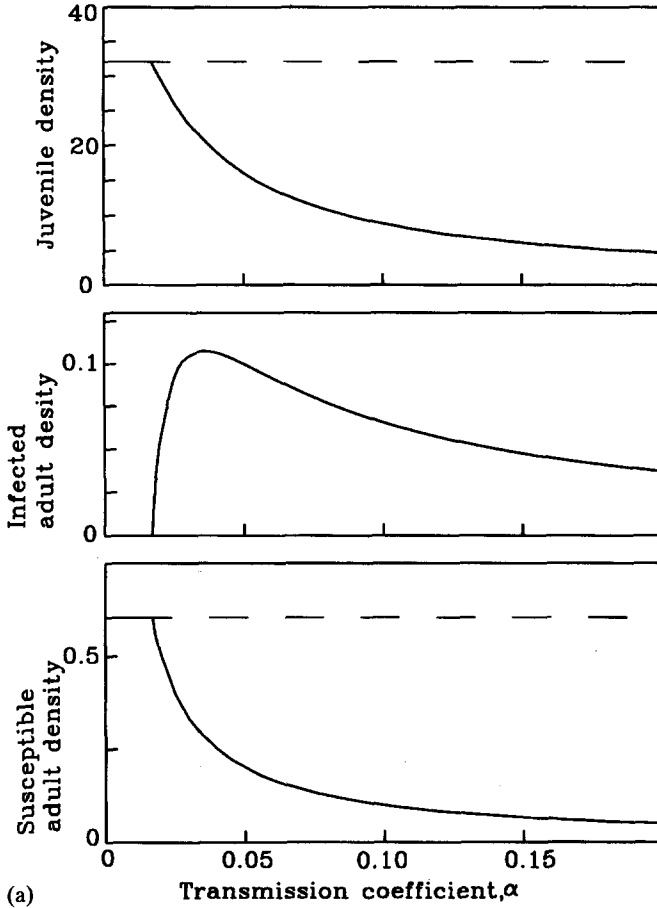
FIG. 1. Steady-state values of the density of juveniles, susceptible adults, and infected adults as a function of the transmission coefficient, α, for the insect-pathogen model with adults susceptible to the disease: (a) $\tau = 400$, $\beta = 0.01$, $\omega_A = \omega_J = 0.01$; (b) $\tau = 85$, $\beta = 0.1$, $\omega_A = \omega_J = 0.01$. Solid lines, stable steady states; dashed lines, unstable steady states. [See Eqs. (13) and (14) for scaling.] In (a) $R_{0,\text{disease}} = 1$ for $\alpha = 0.0165$; in (b) for $\alpha = 0.0266$.

3.3. THE JUVENILE DISEASE

Besides the trivial steady state [Eq. (23)], we find the boundary steady state $(\hat{J}_2, \hat{A}_2, \hat{J}_2) = (\hat{J}_2, \hat{A}_2, 0)$, where $\hat{J}_2$ and $\hat{A}_2$ are given by Equation (21). Interpretations of these steady states are similar to those for the adult disease. The internal steady state is

$$\left(\hat{J}_3, \hat{A}_3, \hat{I}_3\right) = \left(\frac{\beta}{\alpha}, -\ln \omega_A - \omega_J \tau - \alpha \tau \hat{I}_3, \hat{I}_3\right), \tag{28}$$
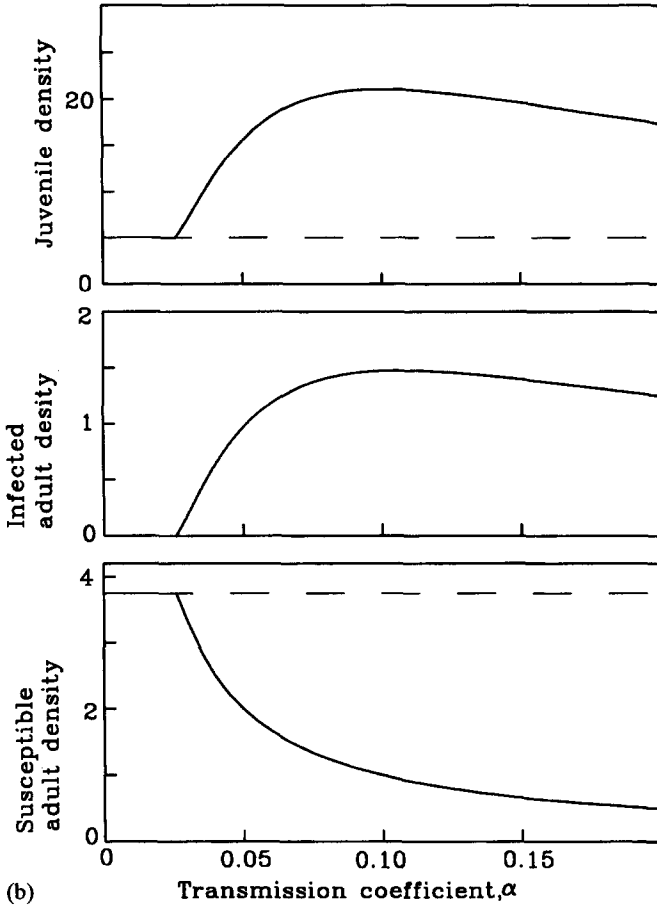
FIG. 1. (*Continued*)

where $\hat{I}_3$ is found from

$$\omega_A\left(-\ln \omega_A - \omega_J\tau - \alpha\tau\hat{I}_3\right)\left(e^{\omega_J\tau + \alpha\tau\hat{I}_3} - 1\right) - \beta\hat{I}_3 - \omega_J\frac{\beta}{\alpha} = 0. \quad (29)$$

Figure 2 shows the boundary and the internal steady state as a function of the transmission coefficient for two sets of values for the other parameters. The internal steady state of I bifurcates either super- or subcritically from the boundary steady state. Both the bifurcation point
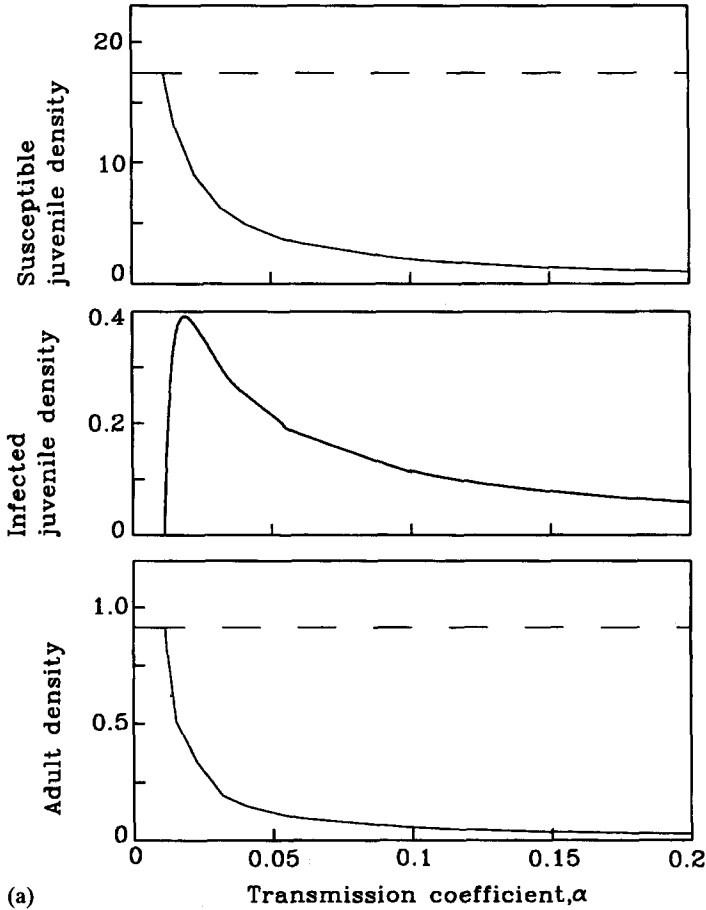
FIG. 2. Steady-state values of the density of susceptible juveniles, infected juveniles, and adults as a function of the transmission coefficient, α, for the insect-pathogen model with juveniles susceptible to the disease: (a) $\tau = 85$, $\beta = 0.1$, $\omega_A = \omega_J = 0.01$; (b) $\tau = 150$, $\beta = 0.2$, $\omega_A = \omega_J = 0.02$. Solid lines, stable steady states; dashed lines, unstable steady states. [See Eqs. (13) and (14) for scaling.]

and the direction of bifurcation again have clear biological interpretations. For small values, $\hat{I}_3$ can be approximated by

$$\hat{I}_3 \approx \frac{\omega_A(-\ln \omega_A - \omega_J \tau)(e^{\omega_J \tau} - 1) - \omega_J \dfrac{\beta}{\alpha}}{\omega_A(\ln \omega_A + \omega_J \tau) \alpha \tau e^{\omega_J \tau} + \omega_A \alpha \tau(e^{\omega_J \tau} - 1) + \beta}, \qquad (30)$$
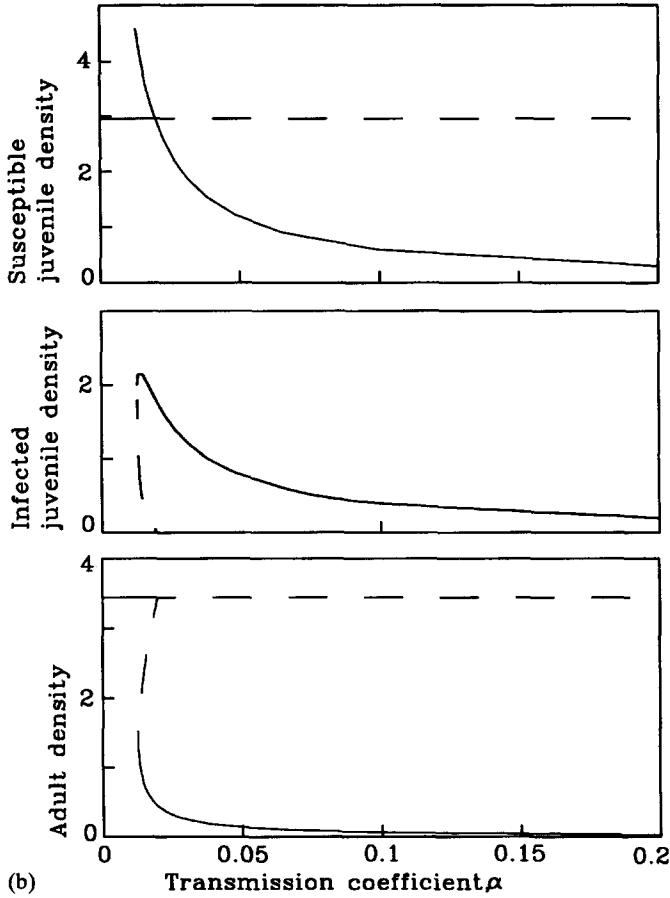
FIG. 2. (*Continued*)

and we find that the internal steady state bifurcates from the boundary steady state at

$$\frac{\omega_A \alpha}{\omega_J \beta}(\ln \omega_A + \omega_J \tau)(1 - e^{\omega_J \tau}) = 1 \quad \Rightarrow \quad \frac{\alpha}{\beta}\hat{J}_2 = 1. \qquad (31)$$

In a population without disease, juvenile density equals $\hat{J}_2$. One infected juvenile produces $\alpha \hat{J}_2$ new infections per unit of time. The average lifetime of an infected juvenile is $1/\beta$. The total number of new infections caused by one newly infected juvenile at infinitesimally low disease density, the $R_{0,\text{disease}} = (\omega_A \alpha / \omega_J \beta)(\ln \omega_A + \omega_J \tau)(1 - e^{\omega_J \tau})$,

therefore equals $(\alpha/\beta)\hat{J}_2$. For $R_{0,\text{disease}} > 1$, an infectious disease can always invade the animal population. From Figure 2, we see, however, that it is, for some parameter combinations, also possible that the internal steady state exists, although $R_{0,\text{disease}} < 1$. At first sight, this seems counterintuitive. However, from Equation (29), we find

$$\frac{d\hat{I}_3}{d\alpha}\bigg|_{R_{0,\text{disease}}=1} = \frac{\omega_J \dfrac{\beta}{\alpha^2}}{\omega_A(\ln \omega_A + \omega_J\tau)\tau e^{\omega_J\tau} + \omega_A\tau(e^{\omega_J\tau}-1) + \dfrac{\beta}{\alpha}}, \quad (32)$$

which implies that the internal steady state bifurcates subcritically (supercritically) if

$$\omega_A(\ln \omega_A + \omega_J\tau)\tau e^{\omega_J\tau} + \omega_A\tau(e^{\omega_J\tau}-1) + \frac{\beta}{\alpha} < (>)0$$

$$\Rightarrow \quad \frac{d\hat{J}_3}{d\hat{I}_3}\bigg|_{R_{0,\text{disease}}=1} > (<)0. \quad (33)$$

When, in a situation where the net-reproductive number of the disease equals unity, an increase in the infected juvenile density results in an increase in the density of susceptible juveniles, the total number of new infections caused by one infected individual becomes larger than unity. In such situations, the disease can invade the animal population. That the juvenile density increases with increasing density of infected juveniles is the result of the hump in the Ricker equation. When part of the juvenile population becomes infected, the adult density will decrease and therewith the population birth rate can increase.

Calculating the total juvenile density, susceptible plus infected, we see that, about $R_{0,\text{disease}} = 1$, the total juvenile density is, for the parameter combinations of Figure 2, larger when disease is present than in the absence of the disease. Clearly, this has consequences for selecting insect pathogens for biological control. We return to this in the discussion.

3.4. THE NONSTAGE STRUCTURED MODEL

Besides the trivial steady state $(S_1, I_1) = (0,0)$ we find the boundary steady state

$$(S_2, I_2) = [\ln(1/\omega), 0] \quad (34)$$

and the internal steady state

$$(S_3, I_3) = \left(\frac{\beta}{\alpha}, \frac{e^{-\frac{\beta}{\alpha}} - \omega}{\alpha}\right). \quad (35)$$

This internal steady state exists, in a biological sense, if

$$\frac{\alpha}{\beta}\ln(1/\omega) > 1. \tag{36}$$

As in the models for adult and juvenile disease, the parameter combination on the left-hand side can be interpreted as $R_{0,\text{disease}}$. Figure 3 shows the boundary steady state and the internal steady state as a function of the transmission coefficient for two sets of values of the other parameters. The internal steady state always bifurcates supercritically from the boundary steady state, as in the adult disease model. For small transmission coefficients, the total insect density increases with increasing transmission coefficient. At intermediate transmission coefficient, insect density reaches a maximum. Increasing the transmission coefficient further decreases total insect density.

4. LOCAL STABILITY OF STEADY STATES

We refer to Bellman and Cooke [23] for an introduction to the stability analysis of delay differential equations. A more biologically oriented outline can be found in Gurney and Nisbet [24].

4.1. *THE INSECT POPULATION WITHOUT INFECTIOUS DISEASE*

Linearizing about the trivial steady state, we find the characteristic equation

$$\left(\omega_J + \lambda\right)\left(e^{-(\omega_J\tau + \lambda\tau)} - \lambda - \omega_A\right) = 0, \tag{37}$$

from which we can conclude that the trivial steady-state is unstable if

$$\frac{e^{-\omega_J\tau}}{\omega_A} > 1 \Leftrightarrow R_{0,\text{insect}} > 1, \tag{38}$$

which implies that the trivial steady state is unstable when the animal population can invade a virgin habitat. The trivial steady state is locally stable if $R_{0,\text{insect}} < 1$. Numerical solutions of the model show that, in this situation, the population dies out independently of parameter values and initial conditions.

Linearizing about the nontrivial steady state yields the characteristic equation

$$\left(\omega_J + \lambda\right)\left[\left(\omega_A\omega_J\tau + \omega_A\ln\omega_A + \omega_A\right)e^{-\lambda\tau} - \lambda - \omega_A\right] = 0. \tag{39}$$
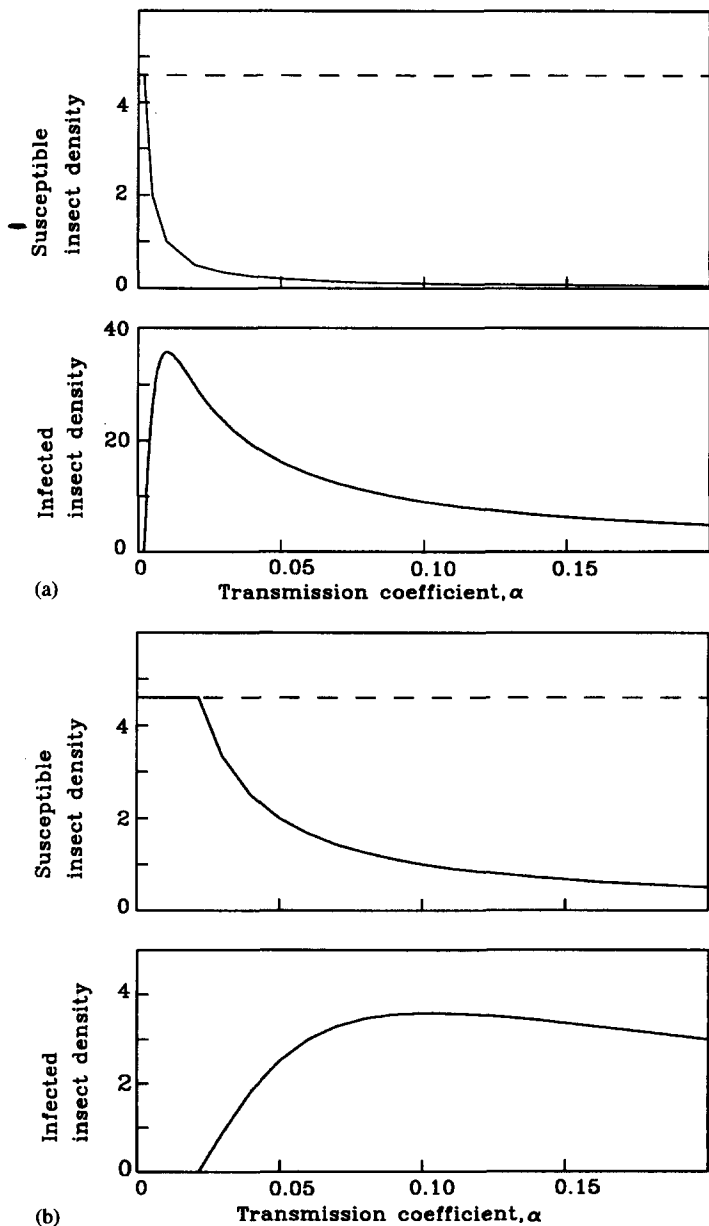
FIG. 3. Steady-state values of the density of susceptible and infected individuals as a function of the transmission coefficient, α, for the nonstage-structured insect-pathogen model: (a) $\tau = 85$, $\beta = 0.1$, $\omega = 0.01$; (b) $\tau = 150$, $\beta = 0.2$, $\omega = 0.02$. Solid lines, stable steady states; dashed lines, unstable steady states. [See Eqs. (13) and (14) for scaling.]

The internal steady state might lose stability through a Hopf bifurcation. Consider a path in a two-dimensional parameter space that intersects the stability boundary. Along this path, a pair of complex conjugate roots crosses the imaginary axis, whereas all other roots lie in the left half-plane. We study this Hopf bifurcation by substituting $\lambda = \theta i$ in Equation (39) and solving the resulting complex equation. This yields

$$\tan(\theta\tau) = -\frac{\theta}{\omega_A}$$

$$\text{where } \theta = \sqrt{\left(\omega_A\omega_J\tau + \omega_A\ln\omega_A + \omega_A^2\right)^2 - \omega_A^2}.$$

(40)

Using Equation (40), we find several curves in parameter space. The branch of internal steady states bifurcates supercritically from the branch of trivial steady states at $R_{0,\text{insect}} = 1$. The trivial steady state is stable for $R_{0,\text{insect}} < 1$ and unstable for $R_{0,\text{insect}} > 1$. The principle of exchange of stability [25] implies that, at such a double point, stability properties of the steady states are exchanged. This implies that the internal steady state is stable for values of $R_{0,\text{insect}}$ larger than but close to unity. Therefore the curve crossed first, if we follow a path through parameter space moving away from the boundary where $R_{0,\text{insect}} = 1$, is the candidate for the stability boundary. Using numerical solutions of Equation (15), we find that this outer curve is indeed the stability boundary. We will use Equation (40) in the stability diagrams of the models with infectious disease.

4.2. THE ADULT DISEASE

Linearizing about the trivial steady state of Equation (23) yields characteristic Equation (37), and this steady state is unstable for the same parameter combinations as those discussed above. Linearizing about the boundary steady state yields the characteristic equation

$$(\lambda + \omega_J)\left(\lambda + \beta - \alpha\hat{A}_2\right)\left[\left(\omega_A\omega_J\tau + \omega_A\ln\omega_A + \omega_A\right)e^{-\lambda\tau} - \lambda - \omega_A\right] = 0.$$

(41)

This characteristic equation has real roots $\lambda = -\omega_J$ and $\lambda = \beta - \alpha\hat{A}_2$. The second eigenvalue lies in the right half-plane when $\alpha\hat{A}_2/\beta > 1$, which also implies that the internal steady state exists by Inequality (25). The third term on the left-hand side of Equation (41) equals the second term of Equation (39), implying Hopf bifurcation for the same parameter values as those in the model without infectious disease. A detailed analysis of the bifurcation structure of this steady state is outside the scope of this paper. Using numerical simulations of the adult disease model, Equation (16), we found that

(1) when $\alpha \hat{A}_2 / \beta > 1$, solutions with $I(0) > 0$ always have positive values for I. This implies that the boundary steady state is unstable when the internal steady state exists.

(2) when the internal steady state does not exist and a pair of complex conjugate roots of Equation (41) lie in the right half-plane, there is a limit cycle in the J, A plane and $I = 0$.

The characteristic equation associated with the internal steady state is

$$
(\lambda + \omega_J)\left[-\lambda\left(1 - \frac{\beta}{\alpha}\right)e^{-\left(\lambda\tau + \frac{\beta}{\alpha} + \omega_J\tau\right)} \right.
$$

$$
\left. + \lambda^2 + (\lambda + \beta)e^{-\left(\frac{\beta}{\alpha} + \omega_J\tau\right)} - \omega_A \beta \right] = 0. \qquad (42)
$$

Substituting $\lambda = \theta i$ in the second part of the left-hand side of Equation (42), we find

$$
\sin(\theta\tau) = \frac{\theta^2 - \beta e^{-\left(\frac{\beta}{\alpha} + \omega_J\tau\right)} + \omega_A \beta}{-\theta\left(1 - \frac{\beta}{\alpha}\right)e^{-\left(\frac{\beta}{\alpha} + \omega_J\tau\right)}},
$$

$$
\cos(\theta\tau) = \frac{1}{1 - \frac{\beta}{\alpha}}, \qquad\qquad (43)
$$

with $\beta / \alpha < 2$. Equation (43) implies that no roots can cross the imaginary axis if $\beta / \alpha > 2$. System (43) is studied numerically. In the results presented, $\omega_A = \omega_J$. We found no qualitatively different phenomena for $\omega_A \neq \omega_J$.

Figure 4 summarizes the results of the linear stability analysis of the various steady states. In the juvenile period τ versus transmission coefficient α parameter plane, solutions of Equations (40) (horizontal lines) and (43) (cloverleaf-shaped area) are plotted. The curve crossing the α-axis depicts parameter combinations where $R_{0,\text{disease}} = 1$. For parameter combinations on the left-hand side of this line, the disease becomes extinct; on the right-hand side, the disease can invade the animal population. In area I, the boundary steady states is stable; in area 2, the boundary steady state is unstable and numerical solutions show that the cyclic behavior of the density of juveniles and susceptible adults and the density of infected adults equals zero. Inside area 3, the internal steady state is unstable, and numerical solutions show cyclic fluctuations in the density of juveniles, susceptible adults, and infected adults. In area 4, the internal steady state is stable.
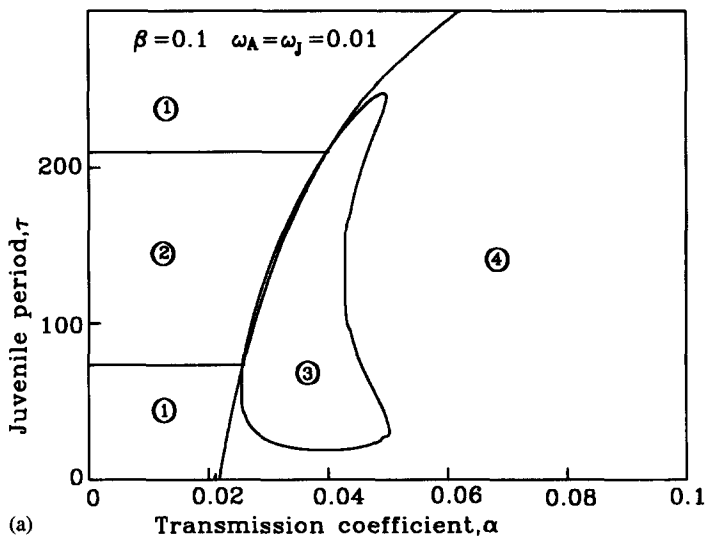
(a)
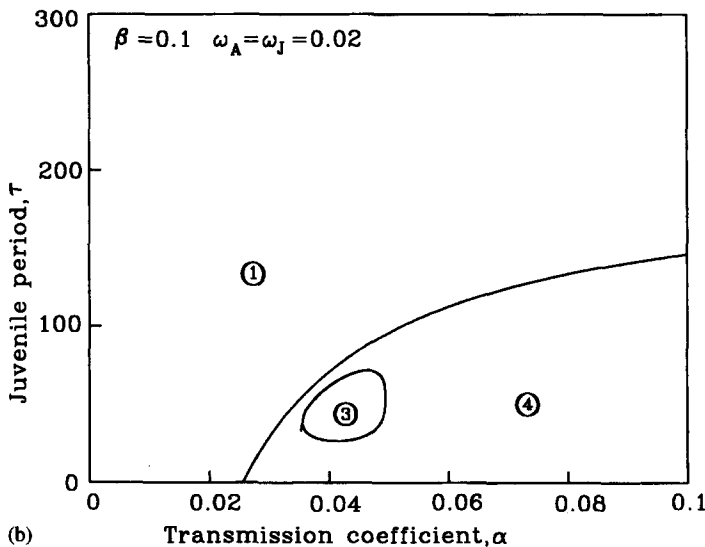
(b)

FIG. 4. Stability diagrams of the insect-pathogen model with adults susceptible to the disease. [For scaling, see Eqs. (13) and (14).] Numbers in figures: (1) Internal steady state does not exist; disease not present. The steady state with juveniles and uninfected adults exists and is stable. (2) Internal steady state does not exist; disease not present. The steady state with juveniles and uninfected adults exists and is unstable. (3) Internal steady state exists; disease present. Internal steady state unstable. (4) Internal steady state exists; disease present. Internal steady state stable.
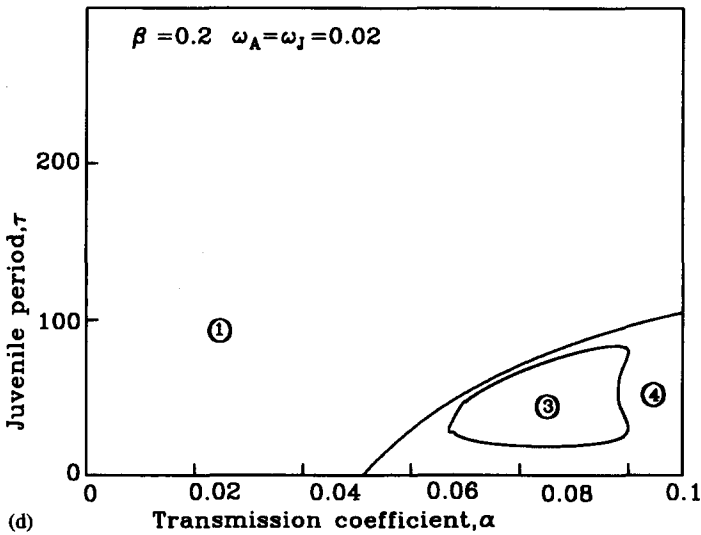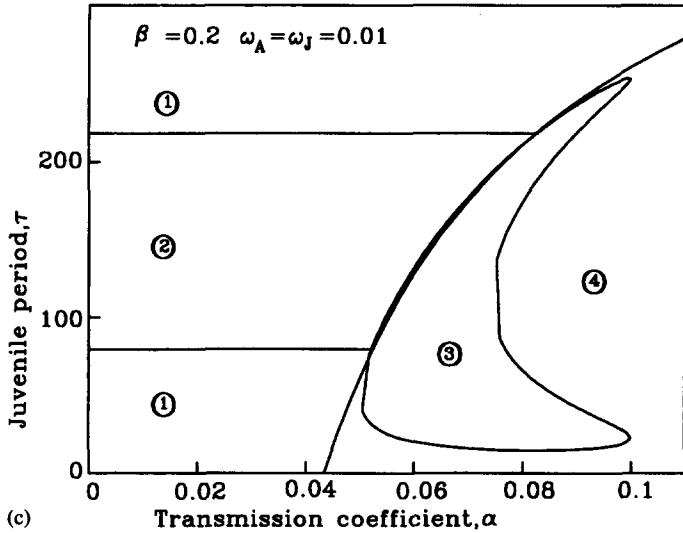
FIG. 4. (*Continued*)

The principle of exchange of stability implies that, for values of the transmission coefficients such that $R_{0,\text{disease}}$ is larger than but close to unity, the stability property of the boundary steady state is transferred to the internal steady state, as is seen in Figure 4. When the internal steady state is stable close to the disease extinction boundary, increasing

the transmission coefficient can result in destabilization of the internal steady state. Further increasing the transmission coefficient will eventually restabilize the internal steady state. When the internal steady state is unstable close to the disease extinction boundary, increasing the transmission coefficient will lead to stabilization. From Equation (43) and Figure 4, we can conclude that the internal steady state is always stable for transmission coefficients larger than $\frac{1}{2}\beta$. Increasing the disease-induced death rate, β, decreases the net-reproductive number of the disease, $R_{0,\text{disease}}$. From Figure 4, we can conclude that increasing β is associated with a larger parameter region where the steady state is unstable.

Small values of β and large values of α are thus stabilizing. This implies that diseases with a large net-reproductive number will lead to constant population densities. Diseases with small and intermediate values of the net-reproductive number can lead either to stable population densities or to cyclic population oscillations. Figure 4 shows that increasing the death rate of the insect leads to smaller parameter areas with cyclic population fluctuations, as is usually found in population dynamic models.

Stability diagrams were also calculated for other parameter values. The qualitative picture of the effects of the transmission coefficient, the juvenile-stage duration, and disease-induced mortality does not seem to be affected by the particular parameter values used in Figure 4.

4.3. THE JUVENILE DISEASE

Linearizing the juvenile disease model [Eq. (17)] proceeds along the same lines as for the other models except for the equation for $P(t)$. To linearize this equation, we substituted $P(t) = \hat{P} + \varepsilon(t)$ and $I(t) = \hat{I} + \phi(t)$, where $\hat{P}$ and $\hat{I}$ are the steady-state values of P and I, respectively, and ε and ϕ are small deviations. This yields

$$\hat{P} + \varepsilon(t) = e^{-\omega_J\tau - \alpha\int_{t-\tau}^{t}(\hat{I}+\phi(\sigma))d\sigma}. \tag{44}$$

Because $\phi \ll 1$, we have

$$\hat{P} + \varepsilon(t) \approx e^{-\omega_J - \alpha\hat{I}\tau}\left[1 - \alpha\int_{t-\tau}^{t}\phi(\sigma)\,d\sigma\right],$$

$$\varepsilon(t) \approx \alpha e^{-\omega_J\tau - \alpha\hat{I}\tau}\int_{t-\tau}^{t}\phi(\sigma)\,d\sigma. \tag{45}$$

Linearizing about the trivial steady state [Eq. (23)] yields characteristic Equation (37), and this steady state is unstable for the same parameter combinations as those discussed above. Linearizing about the

boundary steady state yields the characteristic equation

$$\left(\lambda + \omega_J\right)\left(\lambda + \beta - \alpha\hat{J}_2\right)\left[\left(\omega_A\omega_J\tau + \omega_A\ln\omega_A + \omega_A\right)e^{-\lambda\tau} - \lambda - \omega_A\right] = 0.$$

$$(46)$$

This characteristic equation has real roots $\lambda = -\omega_J$ and $\lambda = \beta - \alpha\hat{J}_2$. The second eigenvalue lies in the right half-plane when $\alpha\hat{J}_2/\beta > 1$, which implies that $R_{0,\text{disease}} > 1$ and the internal steady state exists. Recall, however, that the internal steady state might also exist for parameter values for which $R_{0,\text{disease}} < 1$. The third term on the left-hand side of Equation (46) equals the second term of Equation (39), implying Hopf bifurcation for the same parameter values as those in the model without infectious disease. A detailed analysis of the bifurcation structure of this steady state is outside the scope of this paper. Using numerical simulations, we found that

(1) when the internal steady state exists and $R_{0,\text{disease}} > 1$, solutions, with $I(0) > 0$, always have positive values for $I(t)$. This implies that the boundary steady state is unstable.

(2) when the internal steady state exists and $R_{0,\text{disease}} < 1$, the internal steady state is stable.

(3) when the internal steady state does not exist and a pair of complex conjugate roots lie in the right half-plane, there is a limit cycle in the J, A plane and $I(t) = 0$.

The characteristic equation associated with the internal steady state is

$$\begin{aligned}
&\left\{-\left(\omega_A + \omega_A\ln\omega_A + \omega_A\omega_J\tau + \omega_A\alpha\tau\hat{I}_3\right)\right.\\
&\quad\times\left(\lambda^2 + \omega_J\lambda + \alpha\lambda\hat{I}_3 + \alpha\beta\hat{I}_3\right)e^{-\lambda\tau} + 1\Big\}\\
&\quad\times\left\{\left[\frac{\alpha^2\omega_A}{\lambda}\hat{I}_3\left(\ln\omega_A + \omega_J\tau + \alpha\tau\hat{I}_3\right)\right]\right.\\
&\quad\times\left[\omega_A e^{\omega_J\tau + \alpha\tau\hat{I}_3}\left(1 + \ln\omega_A + \omega_J\tau + \alpha\tau\hat{I}_3\right) - \lambda - \omega_A\right]\Big\} +\\
&\quad + \left(-\lambda - \omega_A\right)\left(\lambda^2 + \omega_J\lambda + \alpha\lambda\hat{I}_3 + \alpha\beta\hat{I}_3\right) = 0.
\end{aligned}$$

$$(47)$$

Substituting $\lambda = \theta i$ we find

$$\begin{aligned}
\sin(\theta\tau) &= \frac{CB - AD}{C^2 + D^2},\\
\cos(\theta\tau) &= \frac{-AC + BD}{C^2 + D^2},
\end{aligned}$$

$$(48)$$

where

$$A = -\theta^4 + \alpha\beta\theta^2\hat{I} + \theta^2\omega_A\omega_J + \alpha\theta^2\omega_A\hat{I}$$
$$+ \alpha^2\omega_A\hat{I}\big[\ln(\omega_A) + \omega_J\tau + \alpha\tau\hat{I}\big]$$
$$\times\left\{\frac{\omega_A}{e^{-\omega_J\tau - \alpha\tau\hat{I}}}\big[1 + \ln(\omega_A) + \omega_J\tau + \alpha\tau\hat{I}\big] - \omega_A\right\},$$

$$B = \theta^3\omega_J + \theta^3\alpha\hat{I} + \theta^3\omega_J - \theta\alpha\beta\omega_A\hat{I} - \hat{I}\theta\alpha^2\omega_A\big[\ln(\omega_A) + \omega_J\tau + \alpha\tau\hat{I}\big],$$

$$C = -\theta^2\omega_A\omega_J - \alpha\theta^2\omega_A\hat{I} - \theta^2\omega_A\omega_J\ln(\omega_A)$$
$$- \alpha\theta^2\hat{I}\omega_A\ln(\omega_A) - \omega_A\omega_J^2\tau\theta^2$$
$$- \omega_A\omega_J\tau\alpha\theta^2\hat{I} - \theta^2\omega_A\omega_J\alpha\tau\hat{I} - \alpha^2\theta^2\omega_A\tau\hat{I}^2$$
$$- \alpha^2\omega_A\hat{I}\big[\ln(\omega_A) + \omega_J\tau + \alpha\tau\hat{I}\big]$$
$$\times\left\{\frac{\omega_A}{e^{-\omega_J\tau - \alpha\tau\hat{I}}}\big[1 + \ln(\omega_A) + \omega_J\tau + \alpha\tau\hat{I}\big] - \omega_A\right\},$$

$$\qquad\qquad\qquad\qquad\qquad\qquad\qquad\qquad (49)$$

$$D = -\omega_A\theta^3 + \alpha\beta\omega_A\theta\hat{I} - \theta^3\omega_A\ln(\omega_A) + \alpha\beta\theta\hat{I}\omega_A\ln(\omega_A) - \omega_A\omega_J\tau\theta^3$$
$$+ \omega_A\omega_J\tau\theta\alpha\beta\hat{I} - \theta^3\alpha\tau\omega_A\hat{I} + \alpha^2\beta\omega_A\tau\theta\hat{I}^2$$
$$+ \alpha^2\omega_A\hat{I}\big[\ln(\omega_A) + \omega_J\tau + \alpha\tau\hat{I}\big]\theta.$$

This set of equations is studied numerically. In the results presented, $\omega_A = \omega_J$. We found no qualitatively different phenomena for $\omega_A \neq \omega_J$.

Figure 5 summarizes the stability analysis for the model of a juvenile disease. In the juvenile period τ versus transmission coefficient α parameter plane, solutions of Equations (48) and (40) are plotted. In area 1, the boundary steady state is stable; in area 2, the boundary steady state is unstable and numerical solutions show cyclic behavior of the density of juveniles and adults in the absence of the disease. In area 3, the internal steady state is unstable, and numerical solutions show cyclic fluctuations in the density of susceptible juveniles, infected juveniles, and adults. In area 4, the internal steady state is stable. In area 5, both the boundary steady state and the internal steady state exist, and the internal steady state is stable.

Comparing Figure 5 with Figure 4, we see that, for juvenile diseases, the effect of parameters α and β on the stability of the internal steady state is opposite to the effect of these parameters for an adult disease. Values of the transmission coefficient and the disease-induced death rate for which the net-reproductive number is close to unity always lead
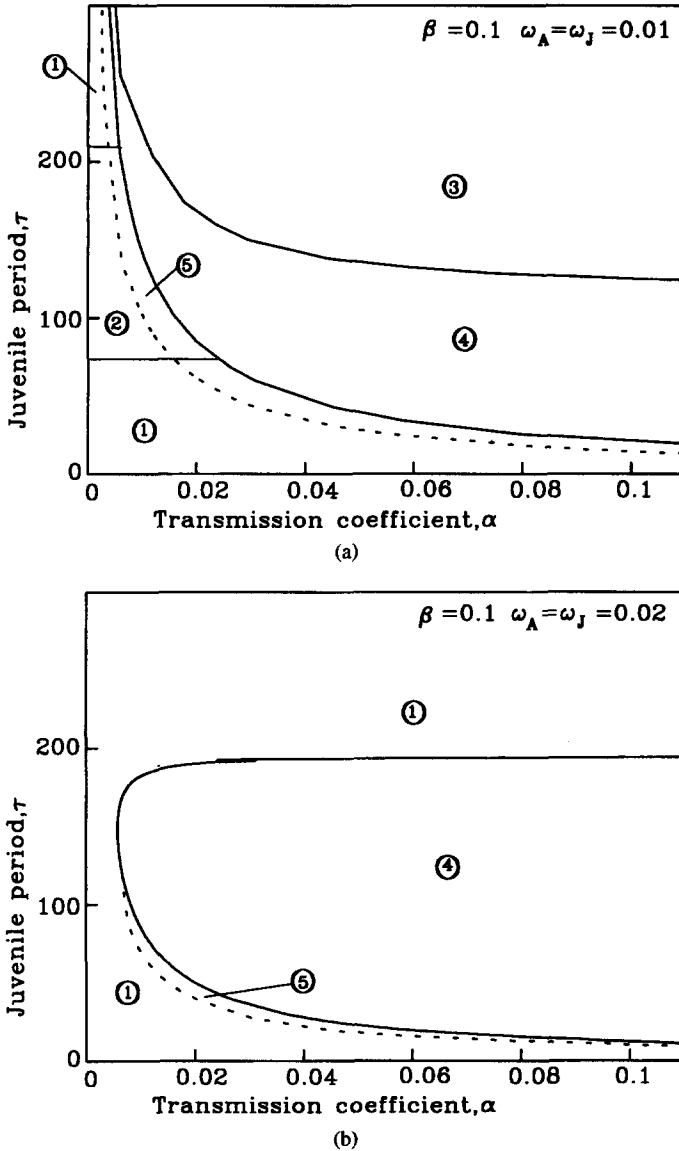
FIG. 5. Stability diagrams of the insect-pathogen model with juveniles susceptible to the disease. [For scaling, see Eqs. (13) and (14).] Numbers in figures 5: (1) Internal steady state does not exist; disease not present. The steady state with uninfected juveniles and adults exists and is stable. (2) Internal steady-state does not exist; disease not present. The steady state with uninfected juveniles and adults exists and is unstable. (3) Internal steady state exists; disease present. Internal steady state unstable. (4) Internal steady state exists; disease present. Internal steady state stable. (5) Depending on initial conditions, disease is present or absent. Internal steady state exists and is stable.
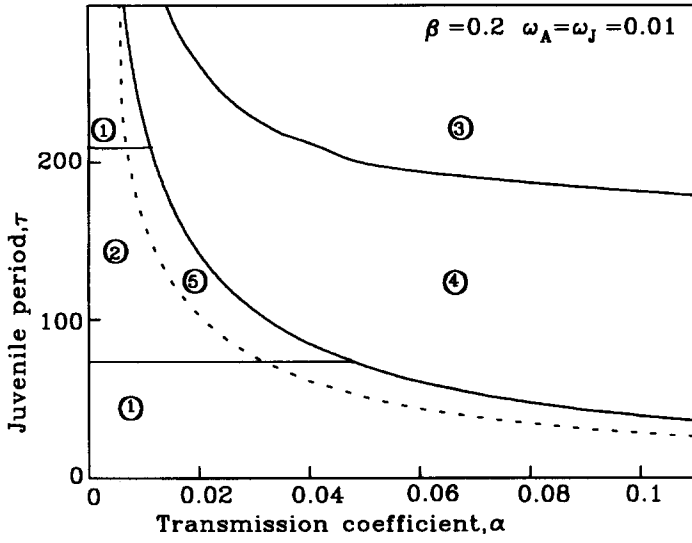
(c)
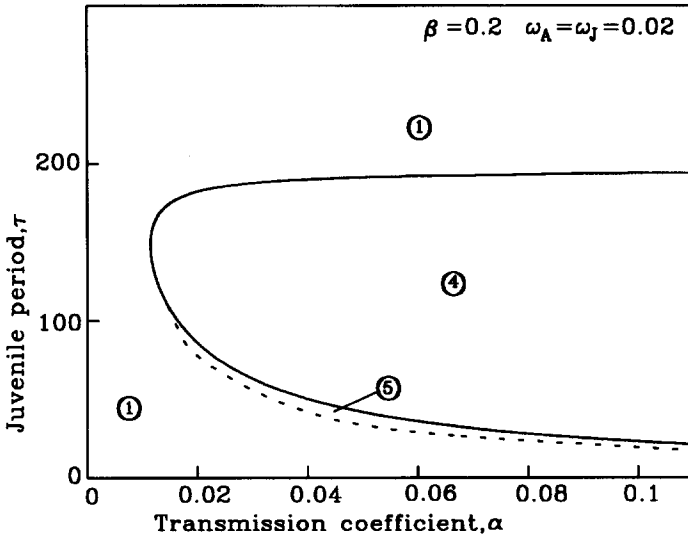
(d)

FIG. 5. (*Continued*)

to stable internal steady states, even when the insect population shows cyclic fluctuations in the absence of the disease. Increasing the transmission coefficient can destabilize the internal steady state; whereas, for an adult disease, increasing α will eventually stabilize the internal steady state.

The effect of the insect death rate on stability corresponds to the usually observed effect, as was found for adult disease.

Stability diagrams were also calculated for other parameter values. The qualitative picture of the effects of the transmission coefficient, the juvenile-stage duration, and disease-induced mortality does not seem to be affected by the particular parameter values used in Figure 5.

4.4. *THE NONSTAGE STRUCTURED MODEL*

Linearizing about the trivial steady state, we find the characteristic equation

$$(1 - \omega - \lambda)(\beta - \lambda) = 0, \tag{50}$$

from which we can conclude that the trivial steady state is unstable if

$$\frac{1}{\omega} > 1. \tag{51}$$

In this unstructured model, $\tau = 0$, and inequality (51) can be interpreted as the condition that the trivial steady state is unstable when $R_{0,\text{insect}} > 1$.

Linearizing about the boundary steady state yields the characteristic equation

$$\left[-\omega \ln(1/\omega) - \lambda \right] \left[\alpha \ln(1/\omega) - \beta - \lambda \right] = 0.$$

This characteristic equation has real roots $\lambda = -\omega \ln(1/\omega)$ and $\lambda = \alpha \ln(1/\omega) - \beta$. The second eigenvalue lies in the right half-plane when $(\alpha/\beta)\ln(1/\omega) > 1$, which is the condition for the existence of an internal steady state. This implies that the boundary steady state is unstable when the internal steady state exists.

Linearizing about the internal steady state yields the characteristic equation

$$\lambda^2 + \frac{\beta}{\alpha} e^{-\frac{\beta}{\alpha}} \lambda + \beta \left(e^{-\frac{\beta}{\alpha}} - \omega \right) = 0.$$

Using the Routh-Hurwitz criteria, we find that the internal steady state is stable if it exists.
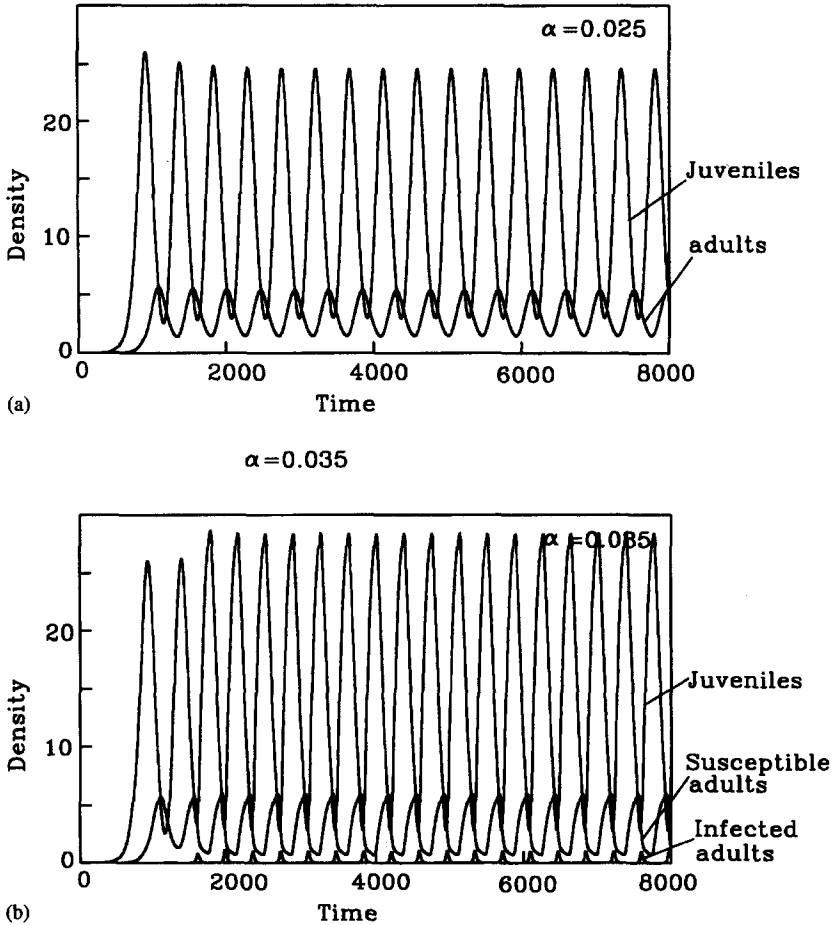
(a)

$\alpha = 0.035$

(b)

FIG. 6. Numerical solutions of the insect-pathogen model with the adults suscep-
tible to the disease. A transect at $\tau = 160$ in the parameter space of Figure 4 (*top
left*) for increasing values of transmission coefficient, α.

5. DYNAMIC BEHAVIOR

The models were numerically solved by using the program SOLVER
[26]. This package is especially developed for the numerical solution of
delay differential equations. The numerical solutions were used to
check the stability boundaries computed in Section 4.

Figures 6 and 7 present solutions of the systems of Equations (16)
and (17). Initial data are $A(t) = J(t) = I(t) = 0$ for $t < 0$, as well as a
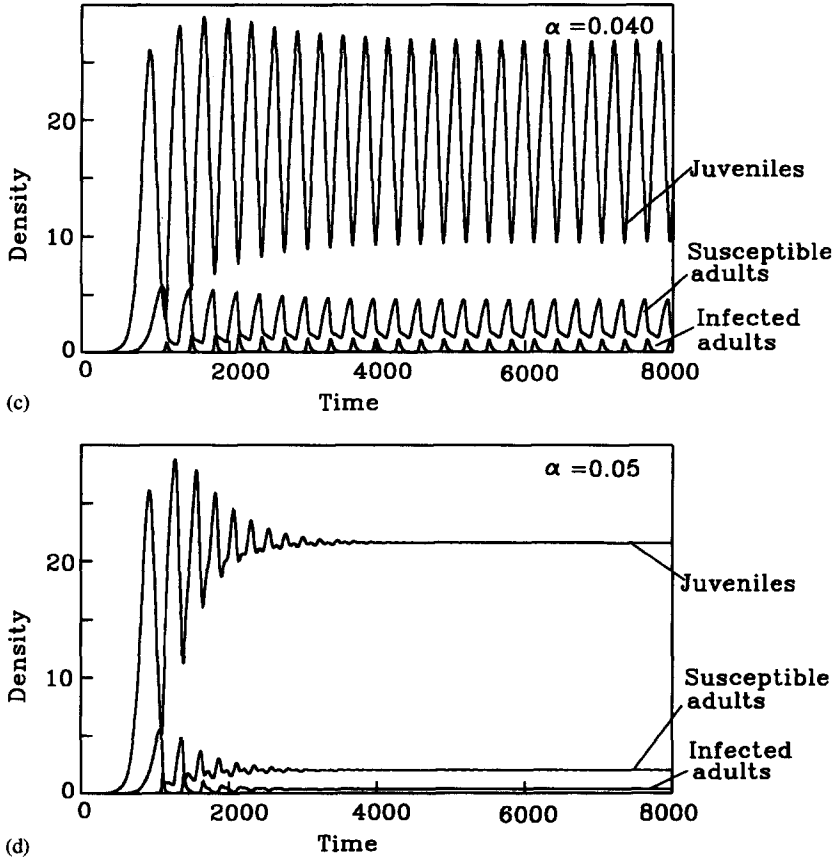short input pulse of newborn individuals and a short input pulse of

(c)

(d)

FIG. 6. (*Continued*)

infected individuals after $t = 0$, for all figures except Figure 7, top left. For Figure 7, top left (dotted lines), the initial condition was $A(t) = 0.9\hat{A}_3$, $J(t) = 0.9\hat{J}_3$, $I(t) = 0.9\hat{I}_3$ for $t \leq 0$. We now consider the period of population cycles in terms of the juvenile period, τ. We will loosely call the juvenile-stage duration the generation time.

The first series (Figure 6) corresponds to a transect at $\tau = 160$ and increasing transmission coefficient, α, in the parameter space of Figure 3, top left. Figure 6 shows the cyclic fluctuations in the density of adults and juveniles in the absence of the disease. Increasing the transmission coefficient to values where the disease can invade the population slightly increases the amplitude of the fluctuations in adult and juvenile density. Further increasing the transmission coefficient decreases the
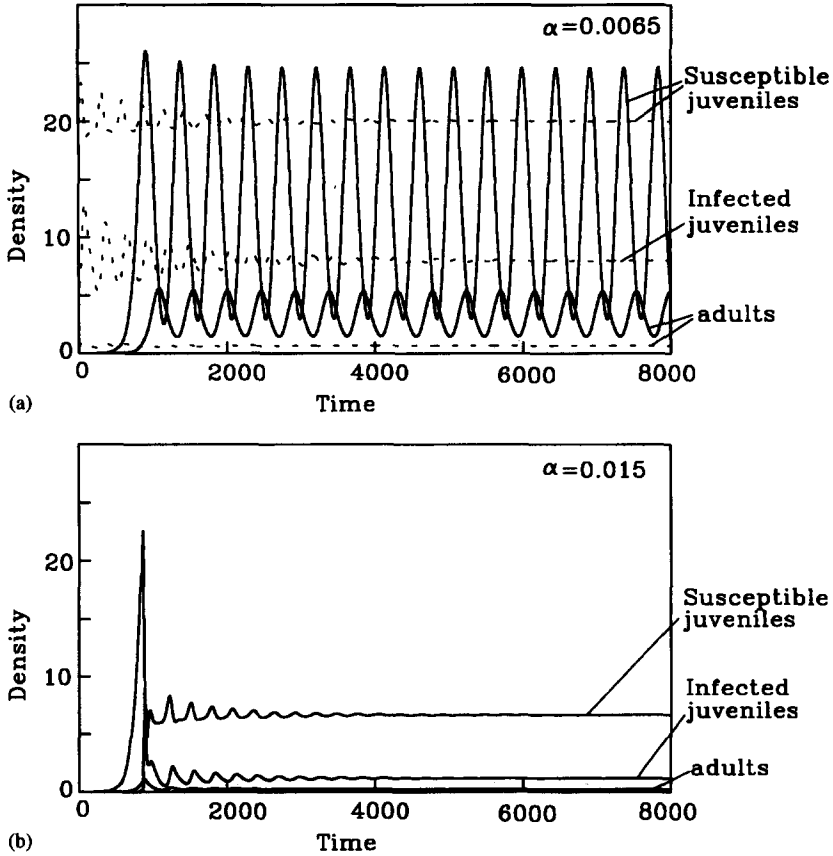
FIG. 7. Numerical solutions of the insect-pathogen model with the juveniles susceptible to the disease. A transect at $\tau = 160$ in the parameter space of Figure 5 (*top left*) for increasing transmission coefficient, α.

amplitude and, for still larger transmission coefficients, the internal steady state becomes stable. The period of the oscillation in the absence of the infectious disease is approximately 2.9 generation times. With the infectious disease present, the period decreases from approximately 2.5 generation times near the extinction boundary of the disease ($R_{0,\text{disease}} = 1$) to about 1.9 generation times near the stability boundary at the right-hand side of the cloverleaf.

The second series (Figure 7) corresponds to a transect at $\tau = 160$ and increasing transmission coefficient, α, in the parameter space of Figure 5, top left. Figure 7 shows the coexistence of a periodic solution without
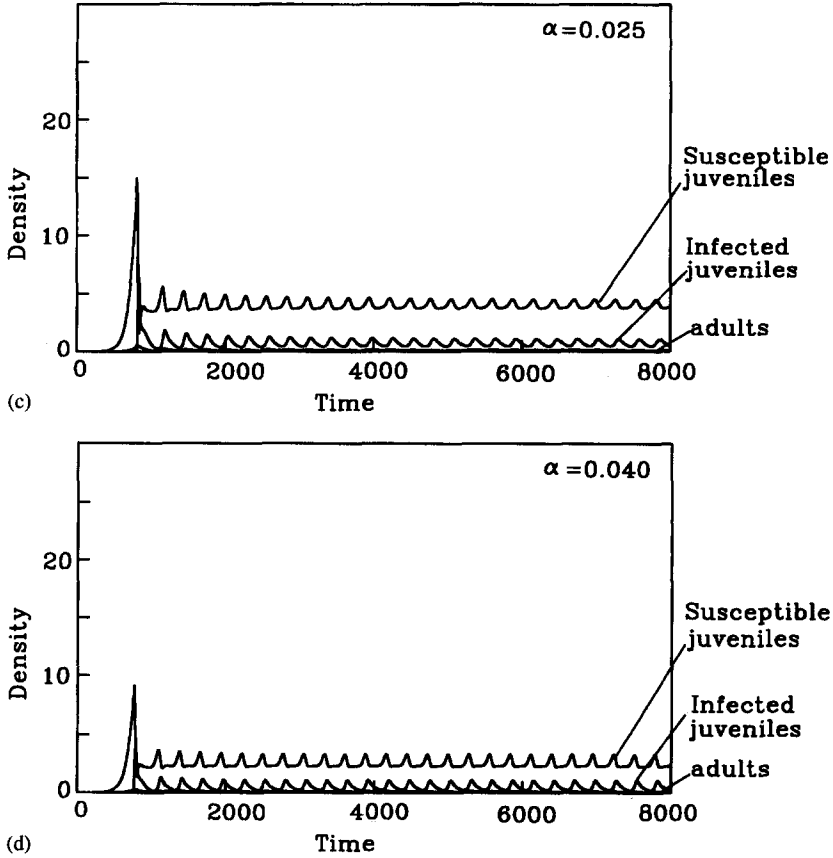
FIG. 7. (*Continued*)

disease and a stable internal steady state when disease is present. If the transmission coefficient is increased, the internal steady state remains stable. Increasing the transmission coefficient further destabilizes the internal steady state, resulting in small-amplitude periodic fluctuations. The period of the fluctuations is smaller in the presence than in the absence of the disease. Close to the stability boundary, the period is approximately 1.6 generation times and slightly increases up to 1.8 generation times for $\alpha = 0.04$. The amplitude of the periodic fluctuations in the presence of a juvenile disease is considerably smaller than the amplitude of the population fluctuations in the absence of the disease. In all our simulation runs, we found only small amplitude fluctuations for the juvenile disease model.

Both series of simulations show that the addition of the insect disease decreases the cycle period compared with the cycle period when no disease is present. We have not been able to find a biological explanation for this phenomenon.

6. DISCUSSION

In this paper, we studied insect-pathogen systems with insect-density dependence and stage-specific susceptibility. For comparison, we also analyzed the nonstage-structured variant. The nonstage-structured variant has one internal steady state. This internal steady state is locally stable if it exists. The coexistence of a stable internal steady state and a boundary steady state in the model for a juvenile disease thus hinges upon the interplay between stage specificity of the disease and the Ricker type of insect-density dependence considered. A biological interpretation of this coexistence of stable steady states is given in the previous sections.

Both the model of an adult disease and the model of a juvenile disease have, for some parameter combinations, an unstable internal steady state. It is shown that, when an unstable internal steady state is present, cyclic population fluctuations arise. Because such cyclic fluctuations are not found in the nonstage-structured model, we can conclude that cycles are the result of both density dependence and stage structure.

Most authors studying the dynamics of insect-pathogen systems, using simple explicit models, used steady-state and stability analysis and numerical solutions in the same way as was done in our study. This enables a comparison between model results. In the comparison, we concentrate on two parameters of the disease process: the transmission coefficient and the disease-induced death rate.

All studies on insect-pathogen systems show the steady-state density to be affected by the transmission coefficient. Increasing the transmission coefficient reduces steady-state insect densities in the absence of insect-density dependence [10, 11, 13, 16]. Bowers et al. [15] show that incorporating logistic-type insect-density dependence results in maximum insect depression at intermediate values of the transmission coefficient. The Ricker-type insect-density dependence used in the present model (nonstructured variant) shows that, for small (large) values of the transmission coefficient, steady-state insect density increases (decreases) with transmission coefficient. Maximal densities are found for intermediate values of the transmission coefficient. We can thus conclude that the effect of the transmission coefficient on steady-state insect density strongly depends on the type of insect-density dependence used. To the conclusion of Bowers et al. [15] and Begon et

al. [14] that insect-density dependence cannot be ignored in the study of insect-pathogen relations, we can add that the precise form of the density dependence also has to be considered.

Adding stage-specific susceptibility further complicates the picture. Whether the use of pathogens is an effective biological control mechanism depends on the insect stage harmful to the crop and on the stage that is susceptible to the disease. With the use of an adult disease, the adult density always decreases with increasing transmission coefficient. Juvenile density can, however, increase when an adult disease is used. Juvenile diseases always decrease steady-state adult density. Juvenile diseases can increase total juvenile density when $R_{0,\text{disease}}$ is close to unity. From these results, we can conclude that the control of insect pests where the adult stage is harmful to the crop is feasible for either an adult or a juvenile disease. The control of insects where the juvenile stage is harmful strongly depends on whether the disease is adult or juvenile and on parameter values of the particular inset-pathogen relation considered. We note here that it is very likely that these conclusions are influenced by the type of insect-density dependence used in the present model study. Other types of density dependence have to be studied in models with stage-dependent susceptibility to get an overview of the various possible effects of the interplay between density dependence and stage-specific susceptibility to get an overview of the various possible effects of the interplay between density dependence and stage-specific susceptibility.

In the models without insect-density dependence and without a free-living infective stage studied by Anderson and May [10, 11] and Brown [16], the transmission coefficient does not affect stability. The same effect of "exploitation efficiency" on stability is found in most host-parasitoid models. Our nonstage-structured model with insect-density dependence also does not show a dependence of stability on the transmission coefficient. This conclusion, however, drastically changes when stage-dependent susceptibility is introduced. Moreover, it is shown that the effect of an increase in transmission coefficient is different for juvenile diseases than for adult diseases. For juvenile disease, increased transmission coefficients promote instability, whereas they promote stability in adult diseases.

The only model study using stage-specific susceptibility published so far is the model by Briggs and Godfray [1]. They show that stage-specific susceptibility strongly affects the dynamics of insect-pathogen systems with transmission through infective units released into the environment. The present model analysis shows that, for diseases transmitted through direct contact between susceptible and infective and for diseases with short-lived infective units, stage-specific susceptibility also has major consequences for the dynamics of insect pathogen relations. Briggs and

Godfray showed that adult insect-pathogen systems show, for many parameter values, persistent cycles with a period of one or a few generation times. Lotka-Volterra–type cycles with a period of more than six generation times are found in small-parameter regions only. For juvenile insect-pathogen systems, the Lotka-Volterra–type cycles are the rule rather than the exception. Cycles with a period of one or a few generations are less common. In the present model with transmission due to direct contact between susceptible and infective, we found, for both juvenile and adult diseases, a cycle period of one or a few generations only. Lotka-Volterra–type cycles have not been found. We can thus conclude that the type of transmission dynamics influences the dynamic behavior of insect pathogen systems.

From the above discussion, we conclude that stage-specific susceptibility has a major effect on steady states and their stability. Moreover, the effect of variations in parameter values can deviate markedly from the effects usually found in models of insect-pathogen systems.

The disease-induced death rate is found to be stabilizing in the models of Anderson and May [11] and Brown [16]. In the model for an adult disease, the parameter area where steady states are unstable increases when the disease-induced death rate increase. For juvenile diseases, an increasing disease-induced death rate is found to be stabilizing. Again, the dynamics of insect-pathogen systems depends essentially on which stage is susceptible to the disease.

In conclusion we can say that stage-specific susceptibility, insect-density dependence, and, especially, the interplay between these two mechanisms strongly affects the dynamics of insect-pathogen relations.

REFERENCES

1   C. J. Briggs and H. C. J. Godfray, The dynamics of insect-pathogen interactions in stage-structured populations. *Am. Nat.* 145, 855–887 (1995).
2   H. D. Burges, *Microbial Control of Pests and Plant Diseases.* Academic Press, London, New York, 1981.
3   T. R. Glare and T. A. Jackson, Eds., *Use of Pathogens in Scarab Past Management.* Intercept Ltd., Andover, Hampshire, UK, 1992.
4   J. R. Fuxa, Ecological considerations for the use of entomopathogens in IPM. *Annu. Rev. Entomol.* 32, 225–251 (1987).
5   A. E. Hajek and R. J. St. Leger, Interactions between fungal pathogens and insect hosts. *Annu. Rev. Entomol.* 39, 293–332 (1994).
6   H. K. Kaya and R. Gaugler, Entomopathogenic nematodes. *Annu. Rev. Entomol.* 38, 181–206 (1993).

7   T. S. Larkin, A. W. Sweeney, and R. I. Carruthers, Simulation of the dynamics of a microbian pathogen of mosquitoes. *Ecol. Model.* 77, 143–165 (1995).

8   J. V. Maddox, The effect of regulations on the use of insect pathogens as biological control agents. In *Regulations and Guidelines: Critical Issues in Biological Control*, R. K. Charudattan and H. W. Browning, Eds., Univ. Florida, Gainesville, 1992.

9   D. W. Onstad and R. I. Carruthers, Epizootiological models of insect diseases. *Annu. Rev. Entomol.* 35, 399–419 (1990).

10 R. M. Anderson and R. M. May, Infectious diseases and population cycles of forest insects. *Science* 210, 658–661 (1980).

11 R. M. Anderson and R. M. May, The popualtion dynamics of microparasites and their invertebrate hosts. *Philos. Trans. R. Soc. Lond. Ser. B* 291, 451–524 (1980).

12 G. Dwyer, Density dependence and spatial structure in the dynamics of insect pathogens. *Am. Nat.* 143, 533–562 (1994).

13 M. E. Hochberg, The potential role of pathogens in biological control. *Nature* 337, 262–265 (1989).

14 M. Begon, R. G. Bowers, N. Kadianakis, and D. E. Hodgkinson, Disease and community structure: the importance of host self-regulation in a host-host-pathogen model. *Am. Nat.* 139, 1131–1150 (1992).

15 R. G. Bowers, M. Begon, and D. E. Hodgkinson, Host-pathogen population cycles in forest insects? Lessons from simple models reconsidered. *Oikos* 67, 529–538 (1993).

16 G. C. Brown, Stability in an insect-pathogen mode incorporating age-dependent immunity and seasonal host reproduction. *Bull. Math. Biol.* 46, 139–153 (1984).

17 J. H. Myers, Can a general hypothesis explain population cycles of forest *Lepidoptera*? *Adv. Ecol. Res.* 18, 179–242 (1988).

18 D. W. Onstad and R. I. Carruthers, Epizootiological models of insect diseases. *Annu. Rev. Entomol.* 35, 399–419 (1990).

19 W. S. C. Gurney, R. M. Nisbet, and J. H. Lawton, The systematic formulation of tractable single-species population models incorporating age structure. *J. Anim. Ecol.* 52, 479–495 (1983).

20 J. R. Beddington, M. P. Hassel, and J. H. Lawton, The components of arthropod predation. *J. Anim. Ecol.* 45, 165–185 (1976).

21 M. P. Hassel, *The Dynamics of Arthopod Predator-Prey Systems*. Princeton Univ. Press, Princeton, NJ, 1978.

22 W. S. C. Gurney, S. P. Blythe, and R. M. Nisbet, Nicholson's blowflies revisited. *Nature* 287, 17–21 (1980).

23 R. Bellman and K. L. Cooke, *Differential-Difference Equations*. Academic Press, New York, 1963.

24 W. S. C. Gurney and R. M. Nisbet, Fluctuation periodicity, generation separation and the expression of larval competition. *Theor. Popul. Biol.* 28, 150–180 (1985).

25 G. Looss and D. D. Joseph, *Elementary Stability and Bifurcation Theory*, Springer-Verlag, New York, Heidelberg, Berlin, 1980.

26 P. Maas, W. S. C. Gurney, and R. M. Nisbet, SOLVER: An adaptable program template for initial value problem solving. Applied Physics Industrial Consultants, Univ. Strathclyde, Glasgow, 1982; revised 1984.